Carbohydrate-functionalized triazolylidene iridium complexes: hydrogenation catalysis in water with asymmetric induction

Joseph P. Byrne,[a] Lidia Delgado,[b] Francesca Paradisi,[a,b] Martin Albrecht[a]*

[a] Dr. J. P. Byrne,[‡] Prof. Dr. F. Paradisi, Prof. Dr. M. Albrecht, Departement für Chemie, Biochemie und Pharmazie, Universität Bern, Freiestrasse 3, 3012 Bern, Switzerland. Email: martin.albrecht@unibe.ch ; Twitter: @albreccht_lab, @ParadisiResLab, @anbeirneach ; URL: https://albrecht.dcbp.unibe.ch

[b] L. Delgado, Prof. Dr. F. Paradisi, School of Chemistry, University of Nottingham, University Park, Nottingham NG7 2RD, UK.

[‡] Present address: School of Chemistry, National University of Ireland Galway, University Road, Galway, Ireland.

Abstract: Two sets of carbohydrate-NHC hybrid iridium complexes were synthesised in order to combine properties of carbohydrates and triazolylidene (trz) ligands in organometallic catalysis. One set features a direct trz linkage to the anomeric carbohydrate carbon, while the second set is comprised of an ethyl linker between the two functional units. The hybrid ligands were prepared by straightforward alkyne azide cycloaddition using carbohydrate azides derived from α-glucose, α-galactose, as well as α- and β-mannose. Deprotection of the carbohydrate was facilitated by the high stability of the Ir–C(trz) bond and afforded hybrid complexes that efficiently catalyse the direct hydrogenation of ketones in water. The catalytic activity of the hybrid complexes was directly influenced by the pH of the aqueous medium and surpassed the activity of carbohydrate-free or acetyl-protected analogues (>90% vs 13% yield). While no enantiomeric induction was observed for the ethyl-linked hybrids, a moderate enantiomeric excess (*ee*) was induced by the directly linked systems (*ee* up to 46% for the β-mannose trz hybrid). The sense of chirality is dictated by the stereochemistry at the anomeric position of the carbohydrate, with α-anomers preferring *R*-products and β-anomers yielding predominantly *S*-enantiomers. Moreover, these carbohydrate-trz hybrid complexes displayed mixed inhibitory activity towards a glycosidase from *H. orenii* that contain a glucose binding site.

Introduction

Carbohydrates constitute an attractive class of compounds for the functionalization of homogeneous catalysts since they impart high water solubility and offer a natural and highly diverse pool for introducing chirality. Remarkably carbohydrates are considerably underexploited in catalysis when compared to other natural chiral pools such as amino acids.[1,2] Pioneering work involving carbohydrate incorporation into phosphine and phosphinite ligands has demonstrated, however, promisingly high enantioselectivities in catalytic olefin hydrogenation.[3–10]

Carbohydrate functionalisation of NHC ligands has been developed only recently,[11] with the majority of research thus far focused towards imidazolylidene ligands and their saturated analogues. Carbohydrate–NHC hybrid complexes have shown anticancer activity,[12] and catalytic activity in Ru-catalysed olefin metathesis reactions,[13] Ir-catalysed alcohol and amine oxidation,[14] and Pd-catalysed Suzuki–Miyaura coupling,[15–17] as well as in Rh-catalysed carbohydrate-directed asymmetric hydrosilylation of ketones.[18,19] Notably, these applications involved fully protected carbohydrate derivatives, and only in Suzuki-Miyaura coupling, in situ deprotection under catalytic conditions has been assumed.[16,17] Our group recently demonstrated that carbohydrate-trz iridium complexes (trz = 1,2,3-triazol-5-ylidene) were sufficiently robust to be deprotected at the carbohydrate site, and that deprotection significantly enhanced the catalytic activity in alcohol and amine oxidation.[14],[20]

The installation of deprotected carbohydrate functionalities on organometallic complexes offers several opportunities. For example, increased solubility in aqueous media allows for using water as a safe, cheap, and abundant solvent[21,22] with the potential to regulate activity through pH modifications, although stability of organometallic systems in buffer solutions is not yet commonplace.[23] These properties paired with sufficiently robust complexes have been exploited to couple organometallic catalysis in tandem with enzymatic transformations,[24–29]

and to build artificial metalloenzymes upon docking of organometallic entities to proteins.[30–32] Similar applications may emerge from carbohydrate-organometallic hybrid systems, since biological receptors for specific carbohydrate bonding are well known, and indeed, carbohydrate-functionalised triazoles were shown to inhibit the activity of glycosidases.[33,34]

Here we demonstrate the incorporation of a variety of carbohydrate motifs into Ir-triazolylidene complexes, and their marked impact on catalytic ketone hydrogenation catalysis, both in terms of activity as well as stereoselectivity. Specifically, the anomeric position was identified to be key for inducing *S*- vs *R*-enantio-preference of the catalyst. Furthermore, bonding of the carbohydrate-trz hybrid complexes to glucose hydrolase was probed to establish the impact of the protein on catalysis.

Results and Discussion

Synthesis of carbohydrate–triazolylidene iridium complexes. Carbohydrate-functionalised triazoles **1** were prepared from phenylacetylene via copper-catalyzed alkyne azide cycloaddition (CAAC) of the corresponding glucose-, galactose, and mannose-azides,[35–37] respectively (Scheme 1). Analogous triazoles **2** with an ethylene spacer between the triazole heterocycle and the carbohydrate unit were synthesized from the corresponding azidoethyl glycopyranosides, which were available via glycosylation of penta-*O*-acetylglycopyranose with bromoethanol and subsequent nucleophilic substitution with NaN_3.[38–40] All compounds **1–2** were obtained in good yields (41–78%). data.[12,14,41]

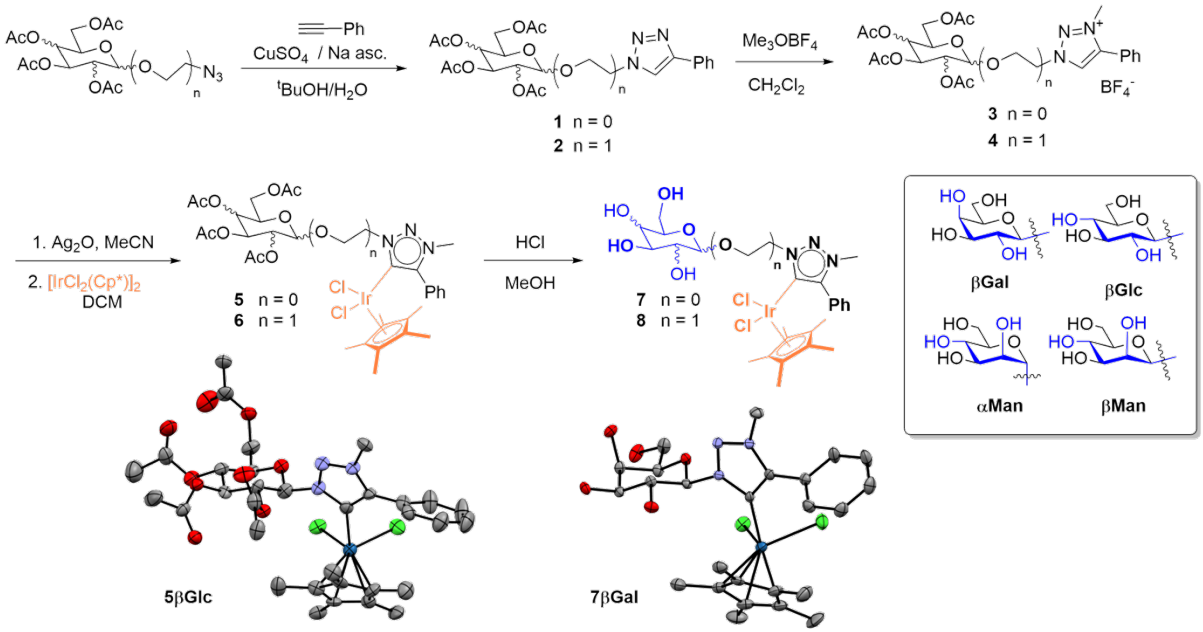

Scheme 1. Synthesis of carbohydrate-functionalized triazolylidene iridium complexes **7** and **8** and crystal structures of **5βGlc** and **7βGal**. (50% probability, hydrogen atoms and CH_3OH molecules co-crystallised with **7βGal** omitted for clarity).

A characteristic singlet at *ca.* 7.9 ppm in each ^{1}H NMR spectrum confirmed formation of the triazole heterocycle. In all compounds, the triazole displayed a single set of ^{1}H NMR resonances, confirming that the products did not undergo anomerisation. Specifically, the anomeric pair **1αMan** and **1βMan**, display different ^{1}H NMR spectra, with distinct coupling constants of the doublet resonance for the anomeric proton of 2.6 Hz (at 6.07 ppm) and 1.4 Hz (at 6.19 ppm), respectively. The resonances arising from the anomeric protons in triazoles **2** were significantly less deshielded than for **1** and, appeared around δ_H 4.5 with a $^3J_{H,H}$ = 7.8 Hz coupling for **2αGlc** and **2αGal**, and 1.6 Hz for **2βMan**. Triazole **1αGal** was deprotected in excellent yields under Zémplen conditions (SI),[33] but attempts to subsequently obtain the corresponding triazolium salt has failed in our hands. Protecting groups were therefore retained for the triazole alkylation and metalation steps.

Near-quantitative alkylation of **1–2** was achieved with $[Me_3O]BF_4$ in CH_2Cl_2 and confirmed by a diagnostic 0.5 ppm downfield shift of the $C_{trz}H$ resonance in the ^{1}H NMR spectrum of the triazolium salt **3** and **4** as well as by HRMS (ESI+) analysis. Reaction of **3–4** with Ag_2O and

transmetallation with $[IrCl_2(Cp^*)]_2$ afforded acetate-protected iridium(III) NHC complexes **5**–**6** in moderate yield (30–48%) after flash chromatography purification. These complexes were characterised by the absence of any downfield resonance in the ^{1}H NMR spectrum and a diagnostic singlet at *ca.* 1.5 ppm corresponding to the Cp* ligand. In **5αMan** and **5βMan**, the ^{1}H NMR resonances of the anomeric proton were broadened and also significantly deshielded by *ca.* 1 ppm with respect to **3αMan** and **3βMan**, indicating electronic perturbation of this site upon metal coordination, similar to **5βGlc** and **5βGal**.[14] By contrast, the resonances for the anomeric proton were essentially unchanged for **6** containing an ethylene spacer between the triazolylidene and carbohydrate moieties (δ_H 4.69–4.84), suggesting no electronic interaction between the carbohydrate and the Ir–triazolylidene unit.

Exposure of the complexes to methanolic NaOMe, *i.e.* typical acetyl deprotection conditions (*vide supra*), led to decomposition of iridium complexes **5**. Since triazolylidene iridium complexes are generally very stable under acidic conditions,[42] the acetyl protecting groups in complexes **5–6** were successfully removed with 0.5 M methanolic HCl.[14] Subsequent precipitation yielded the iridium complexes in good (**7**) to modest (**8**) yields as yellow solids that are air- and moisture stable for several months. The ^{1}H NMR spectra (CD_3OD) of all deprotected iridium complexes contained a single set of resonances, indicating that epimerization at the anomeric position does not occur under these deprotection conditions. All iridium complexes were analysed by a characteristic atomic mass corresponding to the $[M-Cl]^+$ ion by HRMS (ESI+). Moreover, the structure of complex **7βGal** was analyzed by X-ray diffraction on single crystals grown upon diffusion of Et_2O into CH_3OH solution of the complex. The molecular structure confirms the β-configuration and chair conformation of the carbohydrate entity (Scheme 1). As expected for unprotected carbohydrates, the structure features a series of hydrogen bonding interactions between adjacent galactosyl units as well as to co-crystallized MeOH molecules (SI). No intramolecular hydrogen bonding was identified

in the solid state. Bonding geometry about the iridium centre does not deviate significantly from related complex such as **7βGlc**,[14] or related complexes containing a simple triazolylidene ligand.[42]

Interaction of 7βGal with molecular hydrogen. In view of catalytic applications of these iridium complexes, their reactivity towards hydrogen was probed in aqueous solution (H_2O/D_2O 9:1, 40 °C). Exposure of **7βGal** to H_2 induced a notable colour change from pale yellow to dark pink within 15 minutes. Analysis by ^{1}H NMR spectroscopy revealed formation of a new complex which was characterized by a downfield shifted resonance for the Cp–CH_3 groups ($\Delta\delta$ *ca.* 1 ppm, Fig. S.4a–b) and a broad resonance at $\delta_H = -12.8$ integrating for two hydrogens. The spin lattice relaxation time of this latter high-field resonance, T_1 <85 ms,[43] suggests the formation of non-classical hydrides and a Ir–(H_2) complex rather than a classical dihydride.[44,45] This species was stable in solution under ambient conditions for several hours. When analogous experiments were carried out in D_2O solution, the same shift in the Cp* signal was observed, but no high-field resonance was detectable. Instead, deuterium incorporation into the phenyl group of the triazolylidene ligand was observed by the disappearance of ^{1}H resonances in the aromatic region of the ^{1}H NMR spectrum (Fig. S4c–d). These data indicate H/D exchange of the hydride complex with solvent water and reversible cyclometallation of the phenyl group under these conditions.[46,47] We note that water is crucial as a solvent since no hydrogen complex was observed when the reaction was carried out in CH_2Cl_2, EtOH, or MeOH. The carbohydrate functionality is obviously assisting in ensuring water solubility of the iridium complexes, though related unfunctionalized triazolylidene iridium complexes similarly form hydrides.[48] The ability of **7βGal** to bind and activate hydrogen under atmospheric dihydrogen pressures prompts the use of this class of carbohydrate-functionalised NHC complex for application in direct hydrogenation catalysis in aqueous media.

Ketone hydrogenation catalysis in aqueous conditions. The catalytic activity of iridium complex **7βGal** in ketone hydrogenation was assessed by saturating an aqueous solution at various pH with hydrogen gas for 15 minutes, *i.e.* conditions that induce formation of the dihydrogen complex (*vide supra*). Subsequent addition of acetophenone as model substrate induced quantitative conversion to 1-phenylethanol in less than 3 h (40 °C, 1 mol% **7βGal**). Working in aqueous media offers opportunities to optimize the catalytic activity via pH modulation. Therefore, catalytic runs of **7βGal** were conducted at different pH values using various buffer media (Table 1). Under neutral, and even more so under basic conditions, maximum yields were low, reaching only 18% and 35% yield at pH 8.0 and 7.4, respectively (entries 1,2). Precipitation of a yellow solid was also observed at basic pH after a few hours, tentatively attributed to the formation of insoluble hydroxide complexes. The catalytic performance improved considerably at acidic pH. At pH 5.8, conversions reached 74% (entry 3), while further acidification to pH 5.0 gave 94% conversion in 3 h and quantitative conversion after 4 h (entry 4). At pH 3.0, quantitative hydrogenation with **7βGal** was accomplished already within 2 h (entry 5, Fig. S5). Under these conditions, also lower catalyst loadings were active, though at 0.1 mol% **7βGal**, conversions were incomplete even after 24 h and gave a maximum turnover number of 360. These data reveal a clear relationship between pH and both the reaction rate and final product yield, consistent with observations by Ogo *et al.*[49] with Ru-catalysed transfer hydrogenation. This behaviour may be rationalised by an increased stability of the hydride complex combined with substrate activation through proton bonding by the carbonyl group.[22,49]

Table 1. Catalytic acetophenone hydrogenation in aqueous solution buffered at various pH [a]

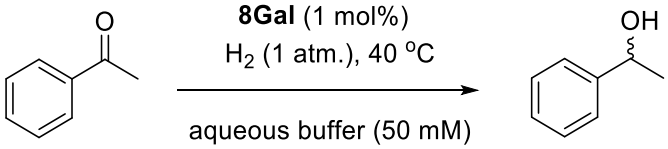

Entry	Complex	pH	Buffer (50 mM)	Yield [b] (3 h; %)	e.e. (%) [c]
1	**7βGal**	8.0	Phosphate	18 [d]	20 (*S*)
2	**7βGal**	7.4	HEPES	35	15 (*S*)
3	**7βGal**	5.8	Phosphate	74	21 (*S*)
4	**7βGal**	5.0	Citrate	94	32 (*S*)
5	**7βGal**	3.0	Citrate	>98	30 (*S*)

[a] General conditions: acetophenone (0.1 mmol), Ir complex (1 µmol, 1 mol%), aqueous buffer (1.0 mL); [b] determined by LCMS with phenol as internal standard; [c] determined by chiral GC; [d] yellow precipitate formed.

While the well-defined stereochemistry of carbohydrates may induce asymmetric catalysis,[3,18,50–53] hydrogenation with **7βGal** induced only a modest enantiomeric excess towards *S*-1-phenylethanol with slight variation upon pH modification. We note that the type of buffer, has a more significant impact on the modest but consistent enantiomeric enrichment of the 1-phenylethanol than the pH. Highest asymmetric induction (30% *ee*) was observed in citrate buffer, while unbuffered conditions (26% *ee*) were less effective, followed by phosphate (20% *ee*) and HEPES buffer (15% *ee*). This dependence suggests that the hydride stabilization by the buffer may be critical for enantiodiscrimination of the substrate.

The impact of the carbohydrate functionality was probed under the optimised conditions, *viz.* citrate buffer at pH 3.0. The catalytic activity of **7βGlc**, **7βMan** and **7αMan** were highly similar to that of **7βGal** and reached >90% conversion within 2 h (Table 2 and Fig. S6). Like **7βGal**, **7βGlc** and **7βMan** led to preferential formation of the *S*-enantiomer with 34% and 46% *ee*, respectively (entries 1–3). The same selectivity of **7βGal** and **7βGlc** suggests that the stereochemistry of the remote C-4 hydroxy group has negligible impact on the chirality transfer, while inversion at C-2 increases the asymmetric induction (**7βGal** *vs* **7βMan**).

Remarkably, **7αMan** showed the opposite enantio-preference and favours the *R*-enantiomer (39% *ee*). This outcome underscores that the NHC-linked carbohydrate scaffold is playing a pivotal role in substrate orientation for asymmetric hydrogen transfer, and that the anomeric configuration is decisive for *S*- *vs R*-preference.

Table 2. Catalytic acetophenone hydrogenation with different iridium complexes. [a]

Entry	Complex	Yield (2h, %) [b]	e.e. (%) [c]
1	**7βGal**	98 (94)	30 (*S*)
2	**7βGlc**	99 (94)	34 (*S*)
3	**7βMan**	90 (86)	46 (*S*)
4	**7αMan**	95 (99)	39 (*R*)
5	**9**	13 (18)	<4
6	**5βGal**	70 (63)	45 (*S*)
7	**5βGlc**	70 (66)	45 (*S*)
8	**5βMan**	55 (69)	34 (*S*)
9	**5αMan**	55 (65)	6 (*S*)
10	**8βGal**	47 (40)	<4
11	**8βGlc**	59 (50)	<4
12	**8αMan**	47 (52)	<4

[a] general conditions: acetophenone (0.1 mmol), Ir complex (1 μmol, 1 mol%), citrate buffer (1.0 mL, 50 mM, pH 3.0), H_2 (1 atm.), 40 °C; [b] yields determined by HPLC relative to phenol as internal standard (in parentheses yields determined by ^{1}H NMR spectroscopy in $CDCl_3$ after product extraction, relative to anisole as internal standard); [c] determined by chiral GC.

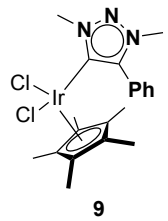

9

Figure 1. Structure of simple triazolylidene complex **9**.

A set of control experiments underpinned the pivotal role of the carbohydrate entity on both catalytic activity and asymmetric induction. Thus, catalytic hydrogenation reaction with **9**, a model iridium complex without carbohydrate functionality (Figure 1), gave very low yield and produced racemic product (Table 3, entry 5). Likewise, complexes **5** containing acetyl-protected carbohydrate units were considerably less active than the analogues with free carbohydrates and reached only 55–70% yield after 2 h (entries 6–9). Remarkably, the acetyl-protected complexes **5βGal** and **5βGlc** induce a higher enantiomeric excess (45%) than their deprotected analogues, while the effect is inverted for the mannose derivatives **5αMan** and **5βMan**. Furthermore, all protected carbohydrate-triazolylidene complexes showed a preference for the *S*-enantiomer, irrespective of the anomeric configuration.

In line with these trends, complexes **8** possessing an ethylene spacer between the deprotected carbohydrate and NHC units gave moderate yields of 47–59% in 2 h and no significant asymmetric induction (entries 10–12). The lack of *ee* is in agreement with the absence of any significant interaction between the carbohydrate and the triazolylidene entities as deduced also by NMR spectroscopy (*vide supra*).

A small substrate scope was carried out with **7βGal** as catalyst precursor (Scheme 2a). Acetophenones substituted with electron-withdrawing nitro and electron-donating methoxy groups were converted with high yields, while an amine substituent impeded catalysis considerably. Cyclohexanone as a representative of aliphatic ketones and also bromobenzaldehyde were reduced under these conditions. Stilbene was inert, suggesting that olefins are not hydrogenated. However, activated olefins in α,β-unsaturated ketones are converted as demonstrated with cinammyl ketone (Scheme 2b). Hydrogenation is considerably slower than with acetophenone with 38% conversion after 2 h and some selectivity towards the saturated ketone intermediate. This selectivity may be a consequence of predominant olefin

reduction or efficient double bond migration.[54] Extension of the reaction time to 16 h yielded predominantly the fully reduced product.

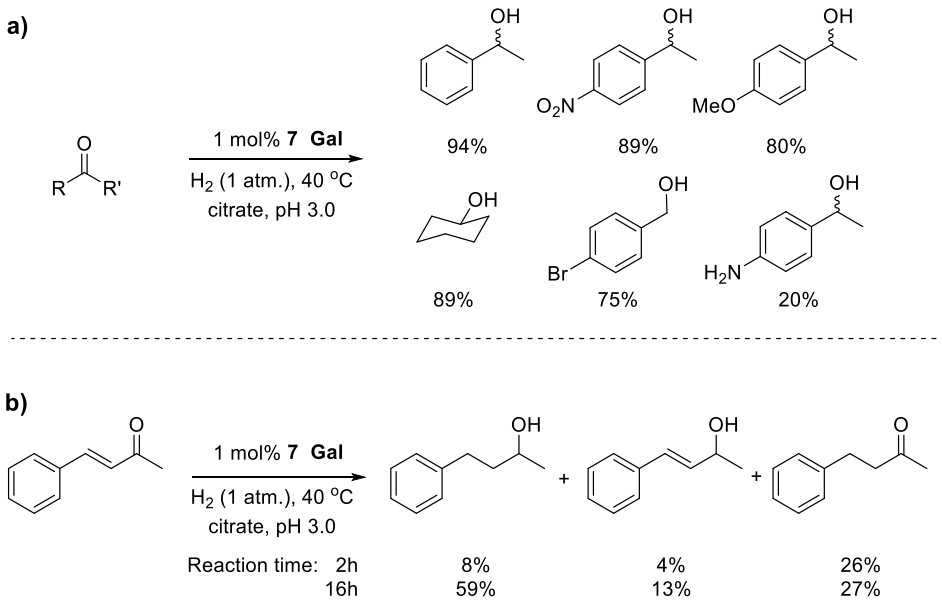

Scheme 2. Products formed by hydrogenation of various substrates. General reaction conditions: substrate (0.1 mmol), **7βGal** (1 μmol, 1 mol%), 1 atm. H_2, 40 °C, citrate buffer (1.0 mL, 50 mM, pH 3.0); yields determined by ^{1}H NMR spectroscopy with anisole as internal standard after 2 h unless stated otherwise.

Interactions of iridium complexes with *H. orenii β*-glucosidase (GH1) enzyme

Further tailoring of activity and selectivity was anticipated by embedding the catalytically active site within a biological scaffold. Specifically, we aimed at using the carbohydrate functionality in complexes **7–8** as anchoring group for interaction with *β*-glucosidase (GH1) enzyme from *H. orenii,* a thermophilic glycosidase containing an active site that is pre-organised to bind and hydrolyse *O*-linked β-glycopyranosides.[55]

Binding of various concentrations of complexes **7–8** was probed by monitoring the enzymatic rate of hydrolysis of *p*-nitrophenyl glucoside by a UV-Vis assay. Essentially complete inhibition (90–98%) was observed with all complexes at 0.5 mM concentration (Fig. S43). Notably, model complex **9** without a carbohydrate functionality showed a similar level

of inhibition, indicating that the loss of enzymatic activity is not limited to the competitive binding of the carbohydrate unit of complexes **7–8** to the GH1 active site.

Inhibition kinetic experiments were carried out for each complex, analysing the activity of the GH1 enzyme in the presence of 0.05 mM of each iridium complex **7–9**. Variations in the reaction parameters with respect to the uninhibited enzyme (Table S2, ESI) indicate that all the complexes behave as 'mixed inhibitors', demonstrating a combination of competitive and non-competitive inhibition processes. Allosteric binding at sites other than the active carbohydrate-binding site is also occurring. Modelled as mixed inhibitors, dissociation constants for both processes were calculated. As expected for a β-glucosidase, the glucose-derived molecules, **7βGlc** and **8βGlc** (K_{ic} = 2.9(5) and 3.4(2) μM, respectively), have higher competitive affinity for the enzyme than the other examples, with **7βGlc** being *ca.* tenfold higher than the uncompetitive affinity.

Catalytic hydrogenation experiments with **7βGal** in the presence of excess GH1 showed no detectable catalytic activity on acetophenone, suggesting that the lack of selective binding prevents these hybrid complexes from assembling into effective artificial metalloenzymes, and the catalyst active site is hindered. Indeed, in catalytic runs with 1 mM solutions of **7βGal** and **7βGlc**, conversion of acetophenone was impacted already in the presence of only 0.3 μM GH1 at pH 7.4 (HEPES 50 mM),[56] achieving about 20% and 15% yield, respectively, *i.e.*, half of the performance recorded in the absence of the enzyme (*cf.* Table 1). Interestingly, catalytic runs in the presence of non-carbohydrate-binding protein BSA also stalled the activity of **7βGal**, indicating a more general role of proteins to hinder this particular reaction. While catalysts **7–8** are bio-compatible and operate under physiologically relevant conditions in aqueous buffer solutions, translation of catalytic activity to biocatalysis through coupling with a protein scaffold still presents a significant challenge. In order to successfully exploit this bio-recognition, stronger and more specific protein-carbohydrate interactions with the

carbohydrate-organometallic hybrid scaffold are required, such as, for example, those exhibited by lectins (e.g. Concanavalin A).[57] Multivalency, where multiple carbohydrate units are presented by a structure, are also well known to increase affinity of compounds for protein carbohydrate-receptor sites.[58] Moreover, variation of the iridium catalytic site, *e.g.* by chelate bonding might shield it from the protein environment to a greater extent and reduce inhibitive interactions.

Conclusions

Carbohydrate-functionalised triazolylidine NHC iridium complexes are efficient pre-catalysts for ketone hydrogenation under mild aqueous conditions and low hydrogen pressures. They significantly outperform carbohydrate-free analogues and acetyl-protected analogues. Direct linkage of the carbohydrate motif to the NHC imparts much higher catalytic benefits compared to ethylene linked more remote carbohydrate trz hybrids. Under optimized conditions at low pH (citrate buffer at pH 3.0), these carbohydrate NHC systems gave essentially quantitative yields for hydrogenation of acetophenone within 2 h. While the carbohydrate entity induced only moderate enantiomeric enrichment up to ~50%, the enantiopreference of the catalyst directly correlates with the stereochemistry at the anomeric carbohydrate position, which offers rational guidelines for further catalyst optimisations. Complexes **7–9** completely inhibited activity of glycosidase enzyme GH1 (*H. orenii*), acting as mixed inhibitors. Kinetic data showed that the glucose-derivatives has the highest competitive binding affinity for GH1, but hydrogenation catalysis was completely impeded by enzyme interactions. More efficient anchoring of the hybrid in the active site may provide a further approach to modulate and increase the catalytic activity and selectivity of these hybrid systems.

Experimental section

General experimental details. 1-α-azido-2,3,4,6-tetra-*O*-acetylmannopyranose was prepared by reaction of penta-*O*-acetylmannopyranose with $TMSN_3$ and $SnCl_4$,[36] while the β-anomer was prepared *via* a glycosyl iodide[37]. 1-azidoethyl-2,3,4,6-tetra-*O*-acetylglycopyranosides,[38–40] **1Glc**[14], **1Gal**[14], **1αMan**,[41] **2Man**,[41] **4Glc**[14], **4Gal**[14], $[IrCl_2Cp^*]_2$[59], **5βGlc**,[14] **5βGal**,[14] **7βGal**,[14] **7βGlc**[14] and **9**[42] were prepared as described previously. Ag_2O was used after regeneration by heating to >160°C under vacuum. Dry, degassed solvents were obtained by filtering over columns of dried aluminium oxide under a positive pressure of argon. Other reagents were obtained from commercial suppliers and used as received. NMR spectra were recorded on Bruker spectrometer operating at room temperature. Chemical shifts (δ in ppm, *J* in Hz) were referenced to residual solvent resonances and are reported downfield from $SiMe_4$. High resolution mass spectrometry and elemental analysis were performed by the Analytical Research Services at University of Bern.

Gas chromatography (GC) was performed on an Agilent 7820A GC System using a CP-Chiralsil-DEXC8 column (25mm × 0.25mm × 0.25μm) as stationary phase. LC analysis was carried out with an Agilent 1260 HPLC system, equipped with a reverse phase XBridge C18 (3.5 μm, 2.1 mm x 30 mm) column, running a gradient method with 0.01% aqueous ammonia and acetonitrile.

Enzyme activity and inhibition assays. In a 96-well plate, 10 μL of enzyme solution, 90 μL of inhibitor solution and 200 μL of *p*-nitrophenyl glucoside solution were added together (to give final concentrations of [*p*-nitrophenyl glucoside] = 10 mM, [HEPES] = 50 mM, pH 7.4). Immediately upon mixing, the assay was begun and formation of *p*-nitrophenol monitored by measuring the formation of the absorbance at 420 nm over 10 minutes. Specific activity

(U/mg) was expressed as μmol of product formed per minute per mg of protein. For inhibition studies [inhibitor] = 0–0.5 mM was used. For inhibition kinetics final concentration of [inhibitor] = 0.05 mM was used.

Catalytic hydrogenation. A 1 mM stock solution of the iridium complex was made up in aqueous buffer. 1 mL of this was transferred to a 10-mL round bottomed flask, before fitting with a rubber septum. The solution was saturated with H_2 for 15 minutes at 40°C. Acetophenone (12 μL, 0.10 mmol) was added and the reaction allowed to proceed under H_2 atmosphere.

To monitor the reaction by LC analysis, phenol added as an internal standard before addition of ketone substrate, and the reaction sampled regularly by syringe. Chiral GC analysis samples were prepared from reactions without phenol and diluted in 2-propanol. In order to determine yield spectroscopically by ^{1}H NMR: after 2h anisole (12 μL, 0.11 mmol), as internal standard, and NaCl (0.3 g) were added and the reaction mixture extracted (0.5 mL ×3) into $CDCl_3$.

Formation of iridium hydride species. 7βGal (5.0 mg, 0.007 mmol) was dissolved in a 9:1 mixture of deionized H_2O and D_2O and was bubbled with H_2 for 15 minutes at 40°C. The ^{1}H NMR spectrum was measured at various temperatures under ambient conditions.

General synthesis of triazoles. The relevant protected azide precursor (1 equiv.), $CuSO_4{\cdot}5H_2O$ (0.4 equiv.) and sodium ascorbate (1 equiv.) were dissolved in aqueous *tert*-butanol solution (1:1 mixture). To this, phenyl acetylene (1 equiv.) was added and (a) stirred at room temperature for 3 days, or (b) heated by microwave irradiation to 100 °C for 6 hours. Reaction mixture was extracted into CH_2Cl_2 and washed with $NH_4Cl_{(aq)}$ (×3), water (×2) and brine (×2), dried over Na_2SO_4, filtered and concentrated under reduced pressure, yielding the triazole as a white or off-white solid. For **2Glc, 2Gal** and **2Man**, a precipitation from Et_2O was necessary to purify the compound.

1βMan. According to the general procedure, 1-β-azido-2,3,4,6-tetra-*O*-acetylmannopyranose (0.270 g, 0.73 mmol), $CuSO_4{\cdot}5H_2O$ (0.073 g, 0.30 mmol), sodium ascorbate (0.146 g, 0.72 mmol) and phenylacetylene (0.08 mL, 0.73 mmol) were reacted. The crude solid was triturated with CH_3OH and filtered, yielding **1βMan** (0.240 g, 0.50 mmol, 70%). Anal. calc. for $C_{22}H_{25}N_3O_9{\cdot}CH_3OH$ (507.498 g/mol), C 54.43, H 5.76, N 8.28%. Found C 54.18, H 6.29, N 8.31%; HRMS (ESI+) Calculated for $C_{22}H_{26}N_3O_9^+$ $[M+H]^+$ *m/z* = 476.1664. Found *m/z* = 476.1650; ^{1}H NMR (400 MHz, $CDCl_3$): δ = 2.00 (s, 3H, $OC(O)CH_3$), 2.05–2.19 (m, 9H, 3 × $OC(O)CH_3$), 4.00 (ddd, 1H, $^3J_{H,H}$ = 10.0, 6.2, 2.3 Hz, mannosyl C^5H), 4.23 (dd, 1H, $^3J_{H,H}$ = 2.3

Hz, $^{2}J_{H,H}$ = 12.5 Hz, mannosyl C^{6}H*H*), 4.37 (dd, 1H, $^{3}J_{H,H}$ = 6.1 Hz, $^{2}J_{H,H}$ = 12.5 Hz, mannosyl C^{6}*H*H), 5.31 (dd, 1H, $^{3}J_{H,H}$ = 10.0, 3.1 Hz, mannosyl C^{3}H), 5.38 (t, 1H, $^{3}J_{H,H}$ = 10.0 Hz, mannosyl C^{4}H), 5.80 (dd, 1H, $^{3}J_{H,H}$ = 3.1, 1.4 Hz, mannosyl C^{2}H), 6.19 (d, 1H, $^{3}J_{H,H}$ = 1.4 Hz, mannosyl C^{1}H), 7.29–7.39 (m, 1H, C$_{Ph}$H), 7.40–7.60 (m, 2H, C$_{Ph}$H), 7.74–7.86 (m, 2H, C$_{Ph}$H), 7.99 (s, 1H, C$_{trz}$H); ^{13}C NMR (100 MHz, $CDCl_3$): δ = 20.5, 20.6, 20.66, 20.74, (4 × OC(O)CH_3), 62.3 (mannosyl C^{6}H$_2$), 65.0 (mannosyl C^{4}H), 68.9 (mannosyl C^{2}H), 70.8 mannosyl C^{3}H), 75.8, (mannosyl C^{5}H), 84.8, (mannosyl C^{1}H), 118.4, (C$_{trz}$H), 125.8, 128.5, 128.9 (3 × C$_{Ph}$H), 130.1 (C$_{Ph}$–trz), 147.8 (C$_{trz}$–Ph), 168.9, 169.6, 169.7, 170.5 (4 × C=O)

2βGlc. According to the general procedure, 1-azidoethyl-2,3,4,6-tetra-*O*-acetylglucopyranoside (0.950 g, 2.30 mmol), $CuSO_4{\cdot}5H_2O$ (0.230 g, 0.92 mmol), sodium ascorbate (0.455 g, 2.30 mmol) and phenylacetylene (0.25 mL, 2.30 mmol) were reacted, yielding **2βGlc** (0.680 g, 1.27 mmol, 55%). Anal. calc. for $C_{24}H_{29}N_3O_{10}{\cdot}0.5(H_2O){\cdot}0.5((C_2H_5)_2O)$ (519.509 g/mol), C 55.22, H 6.24, N 7.43%. Found C 55.48, H 6.75, N 7.54%; HRMS (ESI+) Calculated for $C_{24}H_{29}N_3O_{10}Na^+$ $[M+Na]^+$ *m/z* = 542.1751. Found *m/z* = 542.1727; ^{1}H NMR (300 MHz, $CDCl_3$): δ = 1.72, 1.98, 2,01, 2.07 (4 × s, 3H, OC(O)CH_3), 3.69 (ddd, 1H, $^{3}J_{H,H}$ = 9.5, 4.5, 2.5 Hz, glucosyl C^{5}H), 3.91 (td, 1H, $^{3}J_{H,H}$ = 2.5 Hz, $^{2}J_{H,H}$ = 9.5 Hz, ethylene C*H*H), 4.13 (dd, 1H, $^{3}J_{H,H}$ = 2.5 Hz, $^{2}J_{H,H}$ = 12.4 Hz, glucosyl C^{6}*H*H), 4.21–4.33 (m, 2H, glucosyl C^{6}H*H* and ethylene CH*H*), 4.46 (d, 1H, $^{3}J_{H,H}$ = 7.8 Hz, glucosyl C^{1}H), 4.49–4.75 (m, 2H, ethylene CH_2), 4.97–5.25 (m, 3H, glucosyl C^{2}H, C^{3}H, C^{4}H), 7.27–7.36 (m, 1H, C$_{Ph}$H), 7.37–7.49 (m, 2H, C$_{Ph}$H), 7.80–7.91 (m, 3H, C$_{Ph}$H and C$_{trz}$H); ^{13}C NMR (75 MHz, CD_3OD): δ = 20.4, 20.59, 20.60, 20.7 (4 × OC(O)CH_3), 50.1 (ethylene CH_2), 61.7 (glucosyl C^{6}H$_2$), 67.9 (ethylene CH_2), 68.2 (glucosyl C^{4}H), 70.9 (glucosyl C^{2}H), 72.0 (glucosyl C^{5}H), 72.4 (glucosyl C^{3}H), 100.5 (glucosyl C^{1}H), 121.4 (C$_{trz}$H), 125.7, 128.2, 128.8, 130.5 (4 × C$_{Ph}$), 147.6 (C$_{trz}$–Ph), 169.4, 169.5, 170.1, 170.6 (4 × C=O).

2βGal. According to the general procedure, 1-azidoethyl-2,3,4,6-tetra-*O*-acetylgalactopyranoside (2.03 g, 4.87 mmol), $CuSO_4{\cdot}5H_2O$ (0.486 g, 1.95 mmol), sodium ascorbate (0.965 g, 4.87 mmol) and phenylacetylene (0.53 mL, 4.87 mmol) were reacted, yielding **2βGal** (1.100 g, 2.12 mmol, 43%). Anal. calc. for $C_{24}H_{29}N_3O_{10}{\cdot}0.5(H_2O){\cdot}0.5((C_2H_5)_2O)$ (519.509 g/mol), C 55.22, H 6.24, N 7.43%. Found C 55.45, H 6.66, N 7.30%; HRMS (ESI+) Calculated for $C_{24}H_{30}N_3O_{10}^+$ $[M+H]^+$ *m/z* = 520.1926. Found *m/z* = 520.1937; ^{1}H NMR (300 MHz, $CDCl_3$): δ = 1.70, 1.95, 2,04, 2.14 (4 × s, 3H, OC(O)CH_3), 3.84–3.97 (m, 2H, galactosyl C^{5}H and ethylene CH*H*), 4.01–4.20 (m, 2H, galactosyl C^{6}H$_2$), 4.29 (ddd, 1H, $^{3}J_{H,H}$ = 4.2, 3.0 Hz, $^{2}J_{H,H}$ = 10.1 Hz, ethylene C*H*H), 4.43 (d, 1H, *J* = 7.9 Hz, galactosyl C^{1}H), 4.54 (ddd, 1H, $^{3}J_{H,H}$ = 9.3, 3.0 Hz, $^{2}J_{H,H}$ = 14.5 Hz, ethylene C*H*H), 4.69 (ddd, 1H, $^{3}J_{H,H}$ = 4.2, 3.0 Hz, $^{2}J_{H,H}$ = 14.5 Hz, ethylene CH*H*), 4.95 (dd, 1H, $^{3}J_{H,H}$ = 10.5, 3.5 Hz, galactosyl C^{3}H), 5.21 (dd, 1H, $^{3}J_{H,H}$ = 10.5, 7.9 Hz, galactosyl C^{2}H), 5.38 (dd, 1H, $^{3}J_{H,H}$ = 3.5, 1.1 Hz, galactosyl C^{4}H), 7.27–7.36 (m, 1H, C$_{Ph}$H), 7.38–7.48 (m, 2H, C$_{Ph}$H), 7.79–7.93 (m, 3H, 2 × C$_{Ph}$H and C$_{trz}$H); ^{13}C NMR (75 MHz, CD_3OD): δ = 20.47, 20.54, 20.66, 20.70 (4 × OC(O)CH_3), 50.1 (ethylene CH_2), 61.2 (galactosyl C^{6}H$_2$), 66.9 (galactosyl C^{4}H), 67.8 (ethylene CH_2), 68.5 (galactosyl C^{2}H), 70.6 (galactosyl C^{3}H), 70.8 (galactosyl C^{5}H), 100.9 (galactosyl C^{1}H), 121.6 (C$_{trz}$H), 125.7, 128.1, 128.8, 130.5 (4 × C$_{Ph}$), 147.6 (C$_{trz}$–Ph), 169.7, 170.0, 170.2, 170.4 (4 × C=O).

General synthesis of triazolium salts. The relevant triazole (1 equiv.) and Meerwein's reagent (Me_3OBF_4, 1.1 equiv.) were suspended in dry CH_2Cl_2 (50 mL) and stirred at room temperature for 18 hours. Reaction was quenched with CH_3OH (0.5 mL) and concentrated under reduced pressure, yielding the product, which could be further purified by dissolving in a minimum of CH_2Cl_2 and addition of copious diethyl ether, causing triazolium salts to precipitate as white solid in near-quantitative yields. These compounds were hygroscopic.

3αMan. According to the general procedure, **1αMan** (1.238 g, 2.60 mmol) and Meerwein's reagent (0.414 g, 2.80 mmol) were reacted, yielding **3αMan** (1.550 g, quant.). HRMS (ESI+): Calculated for $C_{23}H_{28}N_3O_9^+$ $[M-BF_4]^+$ *m/z* = 490.1820. Found *m/z* = 490.1799; ^{1}H NMR (300 MHz, $CDCl_3$): δ = 2.04–2.12 (m, 9H, 3 × OC(O)CH_3), 2.18 (s, 3H, OC(O)CH_3 [overlaps with acetone peak]), 4.07–4.56 (m, 6H, N–CH_3, mannosyl C^{6}H$_2$, C^{5}H), 5.35 (t, 1H, $^3J_{H,H}$ = 8.0 Hz, mannosyl C^{4}H), 5.56 (dd, 1H, $^3J_{H,H}$ = 8.0, 3.5 Hz, mannosyl C^{3}H), 6.04 (t, 1H, *J* = 3.5 Hz, mannosyl C^{2}H), 6.47 (d, 1H, $^3J_{H,H}$ = 3.5 Hz, mannosyl C^{1}H), 7.51 – 7.70 (m, 5H, C_{Ph}H), 8.57 (s, 1H, C_{trz}H); ^{13}C NMR (75 MHz, $CDCl_3$): δ = 20.53, 20.55, 20.6, 20.69 (4 × OC(O)CH_3), 39.2 (N–CH_3), 61.2 (mannosyl C^{6}H$_2$), 65.2 (mannosyl C^{4}H), 66.6 (mannosyl C^{3}H), 68.4 (mannosyl C^{2}H), 73.4 (mannosyl C^{5}H), 87.4 (mannosyl C^{1}H), 121.5 (C_{Ph}–trz), 128.4 (C_{trz}H), 129.6, 129.7, 132.1 (3 × C_{Ph}H), 144.5 (C_{trz}–Ph), 169.64, 169.65, 170.0, 170.9 (4 × C=O).

3βMan. According to the general procedure, **1βMan** (0.240 g, 0.46 mmol) and Meerwein's reagent (0.071 g, 0.48 mmol) were reacted, yielding **3βMan** (0.285 g, quant.). HRMS (ESI+): Calculated for $C_{23}H_{28}N_3O_9^+$ $[M-BF_4]^+$ *m/z* = 490.1820. Found *m/z* = 490.1916; ^{1}H NMR (300 MHz, $CDCl_3$): δ = 2.01, 2.12, 2.14, 2.16 (4 × s, 3H, OC(O)CH_3), 4.18–4.38 (m, 6H, N–CH_3, mannosyl C^{5}H, C^6*H*H), 4.45 (dd, 1H, $^3J_{H,H}$ = 5.5 Hz, $^2J_{H,H}$ = 12.9 Hz, mannosyl C^{6}H*H*), 5.37–5.55 (m, 2H, mannosyl C^{3}H, C^{4}H), 6.04 (app s, 1H, mannosyl C^{2}H), 6.53 (app s, 1H, mannosyl C^{1}H), 7.54–7.69 (m, 5H, C_{Ph}H), 8.51 (s, 1H, C_{trz}H); ^{13}C NMR (101 MHz, $CDCl_3$): δ = 20.4, 20.5, 20.6, 20.7 (4 × OC(O)CH_3), 39.0 (N–CH_3), 61.6 (mannosyl C^{6}H$_2$), 64.6 (mannosyl C^{4}H), 67.7 (mannosyl C^{2}H), 70.8 (mannosyl C^{3}H), 75.9 (mannosyl C^{5}H), 86.5 (mannosyl C^{1}H), 121.6 (C_{Ph}–trz), 127.5 (C_{trz}H), 129.6, 129.8, 132.2 (3 × C_{Ph}), 143.6 (C_{trz}–Ph), 169.6, 169.7, 169.8, 170.8 (4 × C=O).

4βGlc. According to the general procedure, **2βGlc** (0.770 g, 1.50 mmol) and Meerwein's reagent (0.244 g, 1.65 mmol) were reacted, yielding **4βGlc** (0.900 g, 1.12 mmol, 74%). Calculated for $C_{25}H_{32}N_3O_{10}^+$ $[M-BF_4]^+$ *m/z* = 534.2064. Found *m/z* = 534.2084; ^{1}H NMR (300 MHz, CD_3OD): δ = 1.94, 1.99 (2 × s, 3H, OC(O)CH_3), 2.02–2.06 (m, 6H, 2 × OC(O)CH_3), 3.77–3.86 (ddd, 1H,$^3J_{H,H}$ = 10.1, 4.4, 2.0 Hz, glucosyl C^{5}H), 4.09–4.44 (m, 7H, N–CH_3, glucosyl C^{6}H$_2$, O–C*H*$_2$–CH_2N), 4.69 (d, 1H, $^3J_{H,H}$ = 7.9 Hz, glucosyl C^{1}H), 2.82–2.98 (m, 3H, O–CH_2–C*H*$_2$N and glucosyl C^{2}H), 5.04 (t, 1H, $^3J_{H,H}$ = 9.5 Hz, glucosyl C^{4}H), 5.22 (t, 1H, *J* = 9.5 Hz, glucosyl C^{3}H), 7.53–7.72 (m, 5H, C_{Ph}H), 8.52 (C_{trz}H); ^{13}C NMR (75 MHz, CD_3OD): δ = 20.57, 20.62, 20.7, (4× OC(O)CH_3 [2×overlapping]), 38.4 (N–CH_3), 54.1 (ethylene CH_2), 61.6 (glucosyl C^{6}H$_2$), 66.6 (ethylene CH_2), 68.1 (glucosyl C^{4}H), 71.2 (glucosyl C^{2}H), 71.9 (glucosyl C^{5}H), 72.5 (glucosyl C^{3}H), 100.6 (glucosyl C^{1}H), 122.0 (C_{Ph}–trz), 129.2 (Ct$_{rz}$H), 129.4, 129.8, 132.0 (3 × C_{Ph}H), 143.2 (C_{trz}–Ph), 169.6, 169.9, 170.0, 170.7 (4 × C=O).

4βGal. According to the general procedure, **2βGal** (0.535 g, 1.03 mmol) and Meerwein's reagent (0.165 g, 1.10 mmol) were reacted, yielding **4βGal** (0.695 g, quant.). Calculated for $C_{25}H_{32}N_3O_{10}^+$ $[M-BF_4]^+$ *m/z* = 534.2064. Found *m/z* = 534.2070; ^{1}H NMR (300 MHz, $CDCl_3$): δ = 1.90, 1.95, 2.04, 2.10 (4 × s, 3H OC(O)CH_3), 3.97 (t, 1H, $^3J_{H,H}$ = 6.5 Hz, galactosyl C^{5}H), 4.01–16 (m, 2H, galactosyl C^{6}H$_2$), 4.17–4.39 (m, 5H, ethylene CH_2, N–CH_3), 4.62 (d, 1H, $^3J_{H,H}$ = 7.6 Hz, galactosyl C^{1}H), 4.76–4.98 (m, 2H, ethylene CH_2), 5.01 (dd, 1H, $^3J_{H,H}$ = 10.4, 3.3 Hz, galactosyl C^{3}H), 5.09 (dd, 1H, $^3J_{H,H}$ = 10.4, 7.6 Hz, galactosyl C^{2}H), 5.38 (dd, 1H, $^3J_{H,H}$ = 3.3, 1.1 Hz, galactosyl C^{4}H), 7.52–7.72 (m, 5H, C_{Ph}H), 8.51 (C_{trz}H); ^{13}C NMR (75 MHz, $CDCl_3$): δ = 20.5, 20.6, 20.7 (4 × OC(O)CH_3 [2×overlapping]), 38.4 (N–CH_3), 54.1 (ethylene CH_2), 61.2 (galactosyl C^{6}H$_2$), 66.2 (ethylene CH_2), 67.0 (galactosyl C^{4}H), 68.7 (galactosyl C^{2}H), 70.5 (galactosyl C^{3}H), 70.9 (galactosyl C^{5}H), 100.9 (galactosyl C^{1}H), 122.1 (C_{Ph}–trz), 129.1 (C_{trz}H), 129.4, 129.8, 132.0 (3 × C_{Ph}H), 143.3 (C_{trz}–Ph), 169.9, 170.1, 170.4, 170.6 (4 × C=O).

4αMan. According to the general procedure, **2αMan** (0.720 g, 1.38 mmol) and Meerwein's reagent (0.209 g, 1.41 mmol) were reacted, yielding **4αMan** (0.840 g, quant.). Calculated for $C_{25}H_{32}N_3O_{10}^+$ $[M-BF_4]^+$ *m/z* = 534.2064. Found *m/z* = 534.2069; ^{1}H NMR (300 MHz, $CDCl_3$): δ = 1.97, 2.02, 2.10, 2.14 (4 × s, 3H, 4 × OC(O)CH_3), 3.87–4.02 (m, 1H, mannosyl C^5H), 4.01–4.37 (m, 8H, N–CH_3, mannosyl C^6H_2 and ethylene CH_2), 4.84 (d, 1H, $^3J_{H,H}$ = 1.8 Hz, mannosyl C^1H), 4.93 (app t, 2H, ethylene CH_2), 5.12 (dd, 1H, $^3J_{H,H}$ = 3.0, 1.8 Hz, mannosyl C^2H), 5.13–5.34 (m, 2H, mannosyl C^2H, C^4H), 7.51–7.71 (m, 5H, $C_{Ph}H$), 8.67 (s, 1H, $C_{trz}H$); ^{13}C NMR (75 MHz, $CDCl_3$): δ = 20.71, 20.75, 20.9 (4× OC(O)CH_3 [2×overlapping]), 38.5 (N–CH_3), 53.6 (ethylene CH_2), 62.4 (mannosyl C^6H_2), 64.6 (ethylene CH_2), 65.8 (mannosyl C^4H), 68.9 (mannosyl C^3H), 69.0 (mannosyl C^2H), 69.1 (mannosyl C^5H), 97.3 (mannosyl C^1H), 121.9 (C_{Ph}–trz), 129.0 (C_{trz}–Ph), 129.5, 129.7, 132.0 (3 × $C_{Ph}H$), 143.7 (C_{trz}–Ph), 169.7, 170.2, 170.3, 170.9 (4 × C=O).

General synthesis of iridium complexes. The relevant triazolium salt (1 equiv.), Ag_2O (0.5 equiv.) and NMe_4Cl (1 equiv.) were suspended in dry CH_3CN (50 mL) and stirred in darkness at room temperature for 18 hours. Crude ^{1}H NMR analysis showed disappearance of the resonance associated with the triazolium CH. The reaction mixture was filtered through a bed of celite and concentrated under reduced pressure. The residue was dissolved in dry CH_2Cl_2 and $[IrCl_2Cp^*]_2$ (0.37 equiv.) added. The reaction was stirred in darkness at room temperature for 18 hours, before cooling over an ice bath, filtering through a bed of Celite and concentrating under reduced pressure, yielding a crude orange solid. This was purified by gradient flash chromatography (SiO_2; CH_2Cl_2–$(CH_3)_2CO$ 0→10%), yielding the product as a yellow solid.

5αMan. According to the general procedure, **3αMan** (1.346 g, 2.33 mmol), Ag_2O (0.278 g, 1.20 mmol), NMe_4Cl (0.254 g, 2.33 mmol) and $[IrCl_2Cp^*]_2$ (0.708 g, 0.89 mmol) were reacted, yielding **5αMan** (0.480 g, 1.07 mmol, 46%). Anal. calc. for $C_{33}H_{42}N_3O_9IrCl_2$ (887.834 g/mol), C 44.64, H 4.77, N 4.73%. Found C 45.08, H 5.18, N 4.39%; HRMS (ESI+) Calculated for $C_{33}H_{42}N_3O_9IrCl^+$ $[M-Cl]^+$ *m/z* = 852.2233. Found *m/z* = 852.2237; ^{1}H NMR (300 MHz, $CDCl_3$): δ = 1.49 (s, 15H, Cp*), 2.02, 2.08, 2.13, 2.24 (4 × s, 3H, OC(O)CH_3), 3.88 (s, 3H, N–CH_3), 4.15–4.44 (m, 3H, mannosyl C^6H_2 and C^5H), 5.43 (t, 1H, $^3J_{H,H}$ = 9.9 Hz, mannosyl C^4H), 5.91 (br s, 1H, mannosyl C^2H), 6.03 (dd, 1H, $^3J_{H,H}$ = 9.8, 3.2 Hz, mannosyl C^3H), 7.42–7.55 (m, 4H, mannosyl C^1H, 3 × $C_{Ph}H$), 7.57–7.67 (m, 2H, $C_{Ph}H$); ^{13}C NMR (75 MHz, $CDCl_3$): δ = 8.6 (Cp* CH_3), 20.7, 20.78, 20.80, 20.9 (4 × OC(O)CH_3), 37.8 (N–CH_3), 62.9 (mannosyl C^6H_2), 66.2 (mannosyl C^4H), 68.6 (mannosyl C^3H), 69.1 (mannosyl C^2H), 72.6 (mannosyl C^5H), 87.2 (mannosyl C^1H), 88.6 (Cp* qt), 127.1, 127.9, 130.2, 132.4 (4 × C_{Ph}), 149.8 (br 2 × C_{trz}), 169.0, 169.7, 170.0, 170.5 (4 × OC(O)CH_3).

5βMan. According to the general procedure, **3βMan** (0.280 g, 0.49 mmol), Ag_2O (0.058 g, 0.25 mmol), NMe_4Cl (0.054 g, 0.49 mmol) and $[IrCl_2Cp^*]_2$ (0.159 g, 0.19 mmol) were reacted, yielding **5βMan** (0.270 g, 0.30 mmol, 62%). Anal. calc. for $C_{33}H_{42}N_3O_9IrCl_2{\cdot}2(H_2O)$ (923.8643 g/mol), C 42.90, H 5.02, N 4.55%. Found C 43.10, H 5.37, N 4.03%; HRMS (ESI+) Calculated for $C_{33}H_{42}N_3O_9IrCl^+$ $[M-Cl]^+$ *m/z* = 852.2233. Found *m/z* =852.2252; ^{1}H NMR (300 MHz, $CDCl_3$): δ = 1.41 (s, 15H, Cp*), 2.04, 2.09, 2.25 (3 × s, 3H, OC(O)CH_3), 3.75 (s, 3H, N–CH_3), 4.16–4.40 (m, 3H, mannosyl C^6H_2, C^5H), 5.14–5.28 (m, 1H, mannosyl C^3H), 5.47 (t, 1H, $^3J_{H,H}$ = 9.9 Hz, mannosyl C^4H), 5.66 (br s, 1H, mannosyl C^2H), 7.40–7.51 (m, 3H, $C_{Ph}H$), 7.56 (br d, 1H,$^3J_{H,H}$ = 0.6 Hz, mannosyl C^1H), 7.76 (br s, $C_{Ph}H$); ^{13}C NMR (75 MHz, $CDCl_3$): δ = 8.8 (Cp* CH_3), 20.6, 20.8, 20.97, 21.04 (4 × OC(O)CH_3), 37.8 (N–CH_3), 62.3 (mannosyl C^6H_2), 65.6 (mannosyl C^4H), 69.4 (mannosyl C^2H), 71.7 (mannosyl C^3H), 75.5 (mannosyl C^5H), 85.6 (mannosyl C^1H), 88.8 (Cp* qt), 127.1, 128.2, 130.2, 132.8 (4 × C_{Ph}), 148.3 (C_{trz}–Ir), 149.3 (C_{trz}–Ph), 169.75, 169.82, 169.9, 170.9 (4 × C=O).

6βGlc. According to the general procedure, **4βGlc** (0.845 g, 1.36 mmol), Ag_2O (0.160 g, 0.69 mmol), NMe_4Cl (0.149 g, 1.36 mmol) and $[IrCl_2Cp^*]_2$ (0.519 g, 0.65 mmol) were reacted, yielding **6βGlc** (0.412 g, 0.66 mmol, 48%). Anal. calc. for $C_{35}H_{46}N_3O_{10}IrCl_2 \cdot 2(H_2O)$ (967.917 g/mol), C 43.43, H 5.21, N 4.34%. Found C 43.73, H 5.30, N 3.79%; HRMS (ESI+) Calculated for $C_{35}H_{46}N_3O_{10}IrCl^+$ $[M-Cl]^+$ *m/z* = 896.2495. Found *m/z* = 896.2518; ^{1}H NMR (300 MHz, $CDCl_3$): δ = 1.40 (s, 15H, Cp* CH_3), 2.00, 2.03, 2.05, 2.09 (4 × s, 3H, OC(O)CH_3), 3.70–3.83 (m, 4H, N–CH_3 and C^5H), 4.14 (dd, 1H, $^3J_{H,H}$ = 2.4 Hz, $^2J_{H,H}$ = 12.3 Hz, glucosyl C^6*H*H), 4.22–4.50 (m, 3H, glucosyl C^6H*H* and ethylene CH_2), 4.71 (br s, 1H, glucosyl C^1H), 4.83–5.16 (m, 4H, glucosyl C^2H, C^4H, and ethylene CH_2), 5.21 (t, 1H, $^3J_{H,H}$ = 9.4 Hz, glucosyl C^3H), 7.35–7.52 (m, 3H, C_{Ph}H), 7.64–7.75 (m, 2H, C_{Ph}H); ^{13}C NMR (75 MHz, $CDCl_3$): δ = 8.8 (Cp* CH_3), 20.6, 20.8, 20.9 (4 × OC(O)CH_3), 37.1 (N–CH_3), 61.9 (CH_2), 62.1 (CH_2), 68.2 (glucosyl C^3H), 68.5 (CH_2), 71.4 glucosyl C^2H, 71.8 (glucosyl C^5H), 72.9 (glucosyl C^4H), 88.2 (Cp* qt), 100.4 (glucosyl C^1H), 127.6, 127.9, 129.9, 132.6 (4 × C_{Ph}), 146.6 (C_{trz}–Ir), 149.0 (C_{trz}–Ph), 169.3, 169.6, 170.2, 170.6 (4 × C=O).

6βGal. According to the general procedure, **4βGal** (0.500 g, 0.80 mmol), Ag_2O (0.093 g, 0.40 mmol), NMe_4Cl (0.087 g, 0.80 mmol) and $[IrCl_2Cp^*]_2$ (0.236 g, 0.30 mmol) were reacted, yielding **6βGal** (0.270 g, 0.28 mmol, 36%). Anal. calc. for $C_{35}H_{46}N_3O_{10}IrCl_2 \cdot (H_2O)$ (949.902 g/mol), C 44.26, H 5.09, N 4.42%. Found C 44.17, H 5.14, N 3.89%; HRMS (ESI+) Calculated for $C_{35}H_{46}N_3O_{10}IrCl^+$ $[M-Cl]^+$ *m/z* = 896.2495. Found *m/z* = 896.2469; ^{1}H NMR (300 MHz, $CDCl_3$): δ = 1.41 (s, 15H, Cp* CH_3), 1.98, 2.06, 2.07, 2.13 (4 × s, 3H, OC(O)CH_3), 3.74 (s, N–CH_3), 3.97 (t, 1H, $^3J_{H,H}$ = 6.7 Hz, galactosyl C^5H), 4.14 (d, 2H, *J* = 6.7 Hz, galactosyl C^6H_2), 4.28–4.42 (m, 2H, ethylene CH_2), 4.69 (br d, 1H, galactosyl C^1H), 4.76–5.23 (br m, 4H, ethylene CH_2 (broad) and galactosyl C^3H, C^2H), 5.41 (dd, 1H, *J* = 3.3, 1.1 Hz, galactosyl C^4H), 7.39–7.50 (m, 3H, C_{Ph}H), 7.63–7.78 (m, 2H, C_{Ph}H); ^{13}C NMR (75 MHz, $CDCl_3$): δ = 8.8 (Cp* CH_3), 20.6, 20.7, 20.8, 21.0 (4 × OC(O)CH_3), 37.1 (N–CH_3), 61.1 (galactosyl C^6H_2), 67.0 (galactosyl C^4H), 68.4 (ethylene CH_2), 68.9 (galactosyl C^2H) ,70.7 (galactosyl C^3H), 70.9 (galactosyl C^5H), 88.2 (Cp* qt), 100.8 (galactosyl C^1H), 127.6, 127.9, 129.9, 132.6 (4 × C_{Ph}), 146.7 (C_{trz}–Ir), 149.0 (C_{trz}–Ph), 169.4, 170.08, 170.12, 170.4 (4 × C=O).

6αMan. According to the general procedure, **4αMan** (0.500 g, 0.80 mmol), Ag_2O (0.093 g, 0.40 mmol), NMe_4Cl (0.087 g, 0.80 mmol) and $[IrCl_2Cp^*]_2$ (0.236 g, 0.30 mmol) were reacted, yielding **6αMan** (0.220 g, 0.23 mmol, 30%). Anal. calc. for $C_{35}H_{46}N_3O_{10}IrCl_2 \cdot (CH_2Cl_2) \cdot 0.5((CH_3)_2CO)$ (961.927 g/mol), C 46.20, H 5.89, N 4.37%. Found C 46.44, H 5.14, N 3.85%; HRMS (ESI+) Calculated for $C_{35}H_{46}N_3O_{10}IrCl^+$ $[M-Cl]^+$ *m/z* = 896.2495. Found *m/z* = 896.2481; ^{1}H NMR (300 MHz, $CDCl_3$): δ = 1.42 (s, 15H, Cp* CH_3), 1.99, 2.04, 2.13, 2.17 (4 × s, 3H, OC(O)CH_3), 3.77 (s, 3H, N–CH_3), 4.00–4.11 (m, 1H, mannosyl C^5H), 4.11–4.44 (m, 4H, ethylene CH_2 and mannosyl C^6H_2), 4.84 (br s, 1H, mannosyl C^1H), 4.93–5.16 (m, 2H, ethylene CH_2), 5.18 (br s, 1H, mannosyl C^2H), 5.21–5.32 (m, 2H, mannosyl C^3H, C^4H), 7.40–7.51 (m, 3H, C_{Ph}H), 7.70–7.86 (m, 2H, C_{Ph}H); ^{13}C NMR (75 MHz, $CDCl_3$): δ = 8.9 (Cp* CH_3), 20.73, 20.75, 20.9, 21.0 (4 × OC(O)CH_3), 37.2 (N–CH_3), 54.0 (ethylene CH_2), 62.4 (mannosyl C^6H_2), 66.1 (ethylene CH_2), 66.5 (mannosyl C^3H) 68.9 (mannosyl C^5H), 69.3 (mannosyl C^2H), 88.2 (Cp* qt), 100.0 (mannosyl C^1H), 127.5, 127.9, 129.8, 132.7 (4 × C_{Ph}), 146.9 (C_{trz}–Ir), 149.2 (C_{trz}–Ph), 169.6, 169.9, 170.3, 170.8 (4 × C=O).

General synthesis of deprotected iridium complexes. The relevant protected iridium complex **5/6** (0.1 mmol) was dissolved in methanolic hydrochloric acid (0.5 M, 2.5 mL) and stood at room temperature overnight. The solution was cooled to −20°C and any precipitate filtered. To the filtrate, copious Et_2O was added and the suspension stored at −20°C for 1 hour. The product was collected as a pale yellow or orange solid upon filtration.

7αMan. According to the general procedure, protected complex **5αMan** (0.100 g, 0.11 mmol) was reacted with methanolic hydrochloric acid (0.5 M, 2.5 mL), yielding **7αMan** (0.052 g, 0.07 mmol, 64%). Anal. calc. for $C_{25}H_{34}N_3O_5IrCl_2{\cdot}2.5(H_2O)$ (784.722 g/mol), C 39.27, H 5.14, N 5.49%. Found C 39.70, H 5.67, N 5.42%; HRMS (ESI+) Calculated for $C_{25}H_{34}N_3O_5IrCl^+$ $[M-Cl]^+$ *m/z* = 684.1811. Found *m/z* = 684.1793; ^{1}H NMR (300 MHz, CD_3OD): δ = 1.44 (s, 15H, Cp* CH_3), 3.66–4.01 (m, 7H, N–CH_3, mannosyl C^6H_2, C^5H, C^4H), 4.26 (br s, 1H, mannosyl C^2H), 4.37 (br s, 1H, mannosyl C^3H), 6.66 (br s, 1H, mannosyl C^1H), 7.41–7.56 (m, 3H, $C_{Ph}H$), 7.60–7.73 (m, 2H, $C_{Ph}H$); ^{13}C NMR (75 Hz, CD_3OD): δ = 7.6 (Cp* CH_3), 36.8 (N–CH_3), 61.8 (mannosyl C^6H_2), 68.3, 71.0, 71.0, 77.7 (5 × mannosyl CH), 88.8 (Cp* qt), 89.5 (mannosyl C^1H), 127.6, 127.7, 129.6, 132.2 (4 × C_{Ph}), 146.6 (C_{trz}–Ir), 148.2 (C_{trz}–Ph).

7βMan. According to the general procedure, protected complex **5βMan** (0.170 g, 0.19 mmol) was reacted with methanolic hydrochloric acid (0.5 M, 2.5 mL), yielding **7βMan** (0.095 g, 0.13 mmol, 68%). Anal. calc. for $C_{25}H_{34}N_3O_5IrCl_2{\cdot}(H_2O)$ (737.700 g/mol), C 40.70, H 4.92, N 5.70%. Found C 40.65, H 5.12, N 5.43%; HRMS (ESI+) Calculated for $C_{25}H_{34}N_3O_5IrCl^+$ $[M-Cl]^+$ *m/z* = 684.1811. Found *m/z* = 684.1822; ^{1}H NMR (300 MHz, CD_3OD): δ = 1.32 (s, 15H, Cp* CH_3), 3.61–3.82 (m, 4H, mannosyl C^5H, C^4H, C^3H, C^6H*H*), 4.00 (app d, 1H, $^3J_{H,H}$ = 11.3 Hz, mannosyl C^6*H*H), 4.09 (s, 3H, N–CH_3), 4.27 (br s, 1H, mannosyl C^2H), 6.03 (br s, 1H mannosyl C^1H), 7.49–7.66 (m, 3H, $C_{Ph}H$), 7.82–7.97 (m, 2H, $C_{Ph}H$); ^{13}C NMR (75 MHz, CD_3OD): δ = 7.8 (Cp* CH_3), 37.0 (N–CH_3), 61.3 (mannosyl C^6H_2), 67.3 (mannosyl C^4H), 71.0 (mannosyl C^2H), 73.0 (mannosyl C^3H), 81.4 (mannosyl C^5H), 86.9 (mannosyl C^1H), 89.0 (Cp* qt), 127.0, 128.7, 130.3, 131.7 (4 × C_{Ph}), 146.2 (C_{trz}–Ir), 146.9 (C_{trz}–Ph).

8βGlc. According to the general procedure, protected complex **6βGlc** (0.250g, 0.27 mmol) was reacted with methanolic hydrochloric acid (0.5 M, 2.5 mL) yielded **8βGlc** (0.042 g, 0.06 mmol, 22%). Anal. calc. for $C_{27}H_{38}N_3O_6IrCl_2{\cdot}(H_2O)$ (781.753 g/mol), C 41.48, H 5.16, N 5.38%. Found C 41.72, H 5.54, N 5.09%; HRMS (ESI+) Calculated for $C_{27}H_{38}N_3O_6IrCl^+$ $[M-Cl]^+$ *m/z* = 728.2078. Found *m/z* = 728.2037; ^{1}H NMR (300 MHz, CD_3OD): δ = 1.41 (s, 15H, Cp* CH_3), 3.18 (t, 1H, $^3J_{H,H}$ = 8.3 Hz, glucosyl C^5H), 3.24–3.41 (m [overlaps with CH_3OH residual peak], 3H, glucosyl C^4H, C^2H, C^3H),), 3.68 (dd, 1H, $^3J_{H,H}$ = 5.1 Hz, $^2J_{H,H}$ = 11.9 Hz, glucosyl C^6*H*H), 3.75–3.99 (m, 4H, N–CH_3 and glucosyl C^6H*H*), 4.25 (br s, 1H, ethylene C*H*H), 4.34–4.54 (m, 2H, ethylene CH*H* and glucosyl C^1H ($^3J_{H,H}$ = 7.80), 5.00 (br s [overlaps with H_2O resonance], 2H, ethylene CH_2), 7.40–7.53 (m, 3H, $C_{Ph}H$), 7.64–7.76 (m, 2H, $C_{Ph}H$); ^{13}C NMR (75 MHz, CD_3OD): δ = 7.7 (Cp* CH_3), 36.4 (N–CH_3), 53.7 (ethylene CH_2), 61.3 (glucosyl C^6H_2), 67.7 (ethylene CH_2), 70.2 (glucosyl C^4H), 73.6 (glucosyl C^3H), 76.7 (glucosyl C^2H), 76.9 (glucosyl C^5H), 88.5 (Cp* qt), 103.1 (glucosyl C^1H), 127.5, 127.9, 129.5, 132.4 (4 × C_{Ph}), 145.9 (C_{trz}–Ir [determined by HMBC]), 148.1 (C_{trz}–Ph).

8βGal. According to the general procedure, protected complex **6βGal** (0.140g, 0.15 mmol) was reacted with methanolic hydrochloric acid (0.5 M, 2.5 mL) yielded **8βGal** (0.053 g, 0.69 mmol, 46%). Anal. calc. for $C_{27}H_{38}N_3O_6IrCl_2{\cdot}1.5(H_2O)$ (790.761 g/mol), C 41.01, H 5.23, N 5.31%. Found C 40.82, H 5.74, N 5.16%; HRMS (ESI+) Calculated for $C_{27}H_{38}N_3O_6IrCl^+$ $[M-Cl]^+$ *m/z* = 728.2078. Found *m/z* = 728.2071; ^{1}H NMR (300 MHz, CD_3OD): δ = 1.42 (s, 15H, Cp* CH_3), 3.41–3.61 (m, 3H, galactosyl C^5H, C^2H, C^3H), 3.69–3.91 (m, 6H, galactosyl C^6H_2, Gal C^4H, N–CH_3), 4.24 (br s, 1H, ethylene C*H*H), 4.37 (d, 1H, $^3J_{H,H}$ = 6.9 Hz, galactosyl C^1H), 4.49 (br s, 1H, ethylene CH*H*), 4.91–5.06 (m [overlaps with H_2O resonance], 2H, ethylene CH_2), 7.39–7.44 (m, 3H, $C_{Ph}H$), 7.63–7.72 (m, 2H, $C_{Ph}H$); ^{13}C NMR (75 MHz, CD_3OD): δ = 7.8 (Cp* CH_3), 36.4 (N–CH_3), 53.7 (ethylene CH_2), 61.1 (galactosyl C^6H_2), 67.8 (ethylene CH_2), 68.9 (galactosyl C^4H), 70.9 (galactosyl C^2H), 73.8 (galactosyl C^3H), 75.3 (galactosyl C^5H), 88.5 (Cp* qt), 103.8 (galactosyl C^1H), 127.5, 127.9, 129.5, 132.4 (4 × C_{Ph}), 145.6 (C_{trz}–Ir), 148.1 (C_{trz}–Ph).

8αMan. Yield = 11%. Anal. calc. for $C_{27}H_{38}N_3O_6IrCl_2 \cdot 2.5(H_2O)$ (808.776 g/mol), C 40.10, H 5.36, N 5.20%. Found C 40.07, H 5.84, N 5.32%; HRMS (ESI+) Calculated for $C_{27}H_{38}N_3O_6IrCl^+$ $[M-Cl]^+$ *m/z* = 728.2078. Found *m/z* = 728.2085; ^{1}H NMR (300 MHz, CD_3OD): δ = 1.41 (s, 15H, Cp* CH_3), 3.43–3.56 (m, 1H, mannosyl C^5H), 3.56–3.67 (m, 2H, mannosyl C^3H, C^4H), 3.68–3.80 (m, 2H, mannosyl C^2H, C^6HH), 3.81–3.94 (m, 4H, N–CH_3, mannosyl C^6HH), 3.93–4.17 (br m, 1H, ethylene C*H*H), 4.43 (br s, 1H, ethylene CH*H*), 4.82–5.07 (m [overlaps with H_2O resonance], 3H, mannosyl C^1H and ethylene CH_2), 7.36–7.58 (m, 3H, $C_{Ph}H$), 7.59–7.76 (m, 2H, $C_{Ph}H$); ^{13}C NMR (75 MHz, CD_3OD) δ 7.7 (Cp* CH_3), 36.5 (N–CH_3), 53.8 (ethylene CH_2), 61.6 (mannosyl C^6H_2), 65.5 (br, ethylene CH_2), 67.0 (mannosyl C^4H), 70.5 (mannosyl C^3H), 71.2 (mannosyl C^2H), 73.7 (mannosyl C^5H), 88.4 (Cp* qt), 100.4 (mannosyl C^1H), 127.5, 127.8, 129.5, 132.5 (4 × C_{Ph}), 145.6 (C_{trz}–Ir [determined by HMBC]), 148.3 (C_{trz}–Ph [determined by HMBC]).

Acknowledgements

We are very grateful to Dr Matteo Planchestainer and Dr René Pretorius for useful discussions. We thank Mr Konrad Uhlmann, Stefan Weissen, and Julien Furrer for technical assistance. This work was financially supported by a Marie Skłodowska-Curie Individual Fellowship (JPB, Grant 749549 'GLYCONHC'), the European Research Council (Grant CoG 615653) and a Royal Society of Chemistry Researcher Mobility Grant (JPB). We thank the group of Chemical Crystallography of the University of Bern (Prof P. Macchi) for the X-ray structure solution and the Swiss National Science Foundation (R'equip project 206021_128724) for co-funding the single crystal X-ray diffractometer at the Departement für Chemie, Biochemie und Pharmazie, Universität Bern.

Supporting Information consisting of supplementary experimental details, crystallographic data, refinement details and further structural analysis, catalytic data, NMR spectra of new compounds, chiral gas chromatograms for *ee* determination, and enzyme inhibition data. CCDC 2142839, 2142842–2142843.

Keywords: aqueous hydrogenation; carbohydrates; iridium; ligand effects; N-heterocyclic carbene

References

[1] T. Wang, X. Han, F. Zhong, W. Yao, Y. Lu, *Acc. Chem. Res.* **2016**, *49*, 1369–1378.

[2] X. Liu, S. Dong, L. Lin, X. Feng, *Chinese J. Chem.* **2018**, *36*, 791–797.

[3] A. S. Henderson, J. F. Bower, M. C. Galan, *Org. Biomol. Chem.* **2016**, *14*, 4008–4017.

[4] S. Castillón, C. Claver, Y. Díaz, *Chem. Soc. Rev.* **2005**, *34*, 702.

[5] S. Woodward, M. Diéguez, O. Pàmies, *Coord. Chem. Rev.* **2010**, *254*, 2007–2030.

[6] M. Diéguez, O. Pàmies, A. Ruiz, S. Castillón, C. Claver, *Tetrahedron: Asymmetry* **2000**, *11*, 4701–4708.

[7] K. Yonehara, K. Ohe, S. Uemura, *J. Org. Chem.* **1999**, *64*, 9381–9385.

[8] M. Diéguez, O. Pàmies, A. Ruiz, S. Castillón, C. Claver, *Chem. – A Eur. J.* **2001**, *7*, 3086–3094.

[9] M. Diéguez, J. Mazuela, O. Pàmies, J. J. Verendel, P. G. Andersson, *J. Am. Chem. Soc.* **2008**, *130*, 7208–7209.

[10] J. Margalef, O. Pàmies, M. Diéguez, *Chem. - A Eur. J.* **2017**, *23*, 813–822.

[11] W. Zhao, V. Ferro, M. V. Baker, *Coord. Chem. Rev.* **2017**, *339*, 1–16.

[12] K. J. Kilpin, S. Crot, T. Riedel, J. A. Kitchen, P. J. Dyson, *Dalton Trans.* **2014**, *43*,

1443–1448.

[13] B. K. Keitz, R. H. Grubbs, *Organometallics* **2010**, *29*, 403–408.

[14] R. Pretorius, J. Olguín, M. Albrecht, *Inorg. Chem.* **2017**, *56*, 12410–12420.

[15] J.-H. Li, W.-J. Liu, Y.-X. Xie, *J. Org. Chem.* **2005**, *70*, 5409–5412.

[16] Y. Imanaka, H. Hashimoto, I. Kinoshita, T. Nishioka, *Chem. Lett.* **2014**, *43*, 687–689.

[17] C. C. Yang, P. S. Lin, F. C. Liu, I. J. B. Lin, G. H. Lee, S. M. Peng, *Organometallics* **2010**, *29*, 5959–5971.

[18] A. S. Henderson, J. F. Bower, M. C. Galan, *Org. Biomol. Chem.* **2014**, *12*, 9180–9183.

[19] A. S. Henderson, J. F. Bower, M. C. Galan, *Org. Biomol. Chem.* **2020**, *18*, 3012–3016.

[20] J. P. Byrne, P. Musembi, M. Albrecht, *Dalton Trans.* **2019**, *48*, 11838–11847.

[21] A. Fernandes, B. Royo, *ChemCatChem* **2017**, *9*, 3912–3917.

[22] Y. Wei, D. Xue, Q. Lei, C. Wang, J. Xiao, *Green Chem.* **2013**, *15*, 629–634.

[23] M. Martínez-Calvo, J. L. Mascareñas, *Coord. Chem. Rev.* **2018**, *359*, 57–79.

[24] A. L. E. Larsson, B. A. Persson, J. E. Bäckvall, *Angew. Chemie Int. Ed. English* **1997**, *36*, 1211–1212.

[25] R. M. Haak, F. Berthiol, T. Jerphagnon, A. J. A. Gayet, C. Tarabiono, C. P. Postema, V. Ritleng, M. Pfeffer, D. B. Janssen, A. J. Minnaard, B. L. Feringa, J. G. De Vries, *J. Am. Chem. Soc.* **2008**, *130*, 13508–13509.

[26] F. G. Mutti, A. Orthaber, J. H. Schrittwieser, J. G. D. Vries, R. Pietschnig, W. Kroutil,

Chem. Commun. **2010**, *46*, 8046–8048.

[27] S. Infante-Tadeo, V. Rodríguez-Fanjul, A. Habtemariam, A. M. Pizarro, *Chem. Sci.* **2021**, *12*, 9287–9297.

[28] R. V. Maaskant, S. Chordia, G. Roelfes, *ChemCatChem* **2021**, *13*, 1607–1613.

[29] S. Bose, A. H. Ngo, L. H. Do, *J. Am. Chem. Soc.* **2017**, *139*, 8792–8795.

[30] V. Köhler, Y. M. Wilson, M. Dürrenberger, D. Ghislieri, E. Churakova, T. Quinto, L. Knörr, D. Häussinger, F. Hollmann, N. J. Turner, T. R. Ward, *Nat. Chem.* **2013**, *5*, 93–99.

[31] F. Schwizer, Y. Okamoto, T. Heinisch, Y. Gu, M. M. Pellizzoni, V. Lebrun, R. Reuter, V. Köhler, J. C. Lewis, T. R. Ward, *Chem. Rev.* **2018**, *118*, 142–231.

[32] H. M. Key, P. Dydio, D. S. Clark, J. F. Hartwig, *Nature* **2016**, *534*, 534–537.

[33] L. L. Rossi, A. Basu, *Bioorg. Med. Chem. Lett.* **2005**, *15*, 3596–3599.

[34] S. Dedola, D. L. Hughes, S. A. Nepogodiev, M. Rejzek, R. A. Field, *Carbohydr. Res.* **2010**, *345*, 1123–1134.

[35] K. L. Cosgrove, P. V. Bernhardt, B. P. Ross, R. P. McGeary, *Aust. J. Chem.* **2006**, *59*, 473.

[36] H. Paulsen, Z. Györgydeák, M. Friedmann, *Chem. Ber.* **1974**, *107*, 1568–1578.

[37] M. Farrell, J. Zhou, P. V. Murphy, *Chem. - A Eur. J.* **2013**, *19*, 14836–14851.

[38] W. Hayes, H. M. . Osborn, S. D. Osborne, R. A. Rastall, B. Romagnoli, *Tetrahedron* **2003**, *59*, 7983–7996.

[39] C. Kieburg, K. Sadalapure, T. K. Lindhorst, *European J. Org. Chem.* **2000**, *2000*, 2035–2040.

[40] L. Gu, P. G. Luo, H. Wang, M. J. Meziani, Y. Lin, L. M. Veca, L. Cao, F. Lu, X. Wang, R. A. Quinn, W. Wang, P. Zhang, S. Lacher, Y.-P. Sun, *Biomacromolecules* **2008**, *9*, 2408–2418.

[41] S. Lal, S. Díez-González, *J. Org. Chem.* **2011**, *76*, 2367–2373.

[42] A. Petronilho, M. Rahman, J. A. Woods, H. Al-Sayyed, H. Müller-Bunz, J. M. Don MacElroy, S. Bernhard, M. Albrecht, *Dalton Trans.* **2012**, *41*, 13074.

[43] Determined at 278 K (300 MHz). The minimum value of T_1 could not be determined accurately because of the freezing point of water.

[44] R. H. Crabtree, *Acc. Chem. Res.* **1990**, *23*, 95–101.

[45] G. E. Dobereiner, A. Nova, N. D. Schley, N. Hazari, S. J. Miller, O. Eisenstein, R. H. Crabtree, *J. Am. Chem. Soc.* **2011**, *133*, 7547–7562.

[46] K. F. Donnelly, R. Lalrempuia, H. Müller-Bunz, M. Albrecht, *Organometallics* **2012**, *31*, 8414–8419.

[47] R. Corberán, M. Sanaú, E. Peris, *J. Am. Chem. Soc.* **2006**, *128*, 3974–3979.

[48] A. Mollar-Cuni, J. P. Byrne, P. Borja, C. Vicent, M. Albrecht, J. A. Mata, *ChemCatChem* **2020**, *12*, 3746–3752.

[49] S. Ogo, T. Abura, Y. Watanabe, *Organometallics* **2002**, *21*, 2964–2969.

[50] M. T. Reetz, T. Neugebauer, *Angew. Chemie Int. Ed.* **1999**, *38*, 179–181.

[51] M. Guitet, P. Zhang, F. Marcelo, C. Tugny, J. Jiménez-Barbero, O. Buriez, C. Amatore, V. Mouriès-Mansuy, J. P. Goddard, L. Fensterbank, Y. Zhang, S. Roland, M. Ménand, M. Sollogoub, *Angew. Chemie - Int. Ed.* **2013**, *52*, 7213–7218.

[52] J. F. Moya, C. Rosales, I. Fernández, N. Khiar, *Org. Biomol. Chem.* **2017**, *15*, 5772–5780.

[53] M. Coll, O. Pàmies, M. Diéguez, *Adv. Synth. Catal.* **2014**, *356*, 2293–2302.

[54] S. Horn, C. Gandolfi, M. Albrecht, *Eur. J. Inorg. Chem.* **2011**, *2011*, 2863–2868.

[55] N. Hassan, T. H. Nguyen, M. Intanon, L. D. Kori, B. K. C. Patel, D. Haltrich, C. Divne, T. C. Tan, *Appl. Microbiol. Biotechnol.* **2014**, *99*, 1731–1744.

[56] Dialysis of GH1 enzyme into buffers in the pH range where **7βGal** gave the best yields of 1-phenylethanol (pH 3–5) resulted in irreversible protein precipitation and denaturing.

[57] S. Mandal, R. Das, P. Gupta, B. Mukhopadhyay, *Tetrahedron Lett.* **2012**, *53*, 3915–3918.

[58] A. Bernardi, J. Jiménez-Barbero, A. Casnati, C. De Castro, T. Darbre, F. Fieschi, J. Finne, H. Funken, K.-E. Jaeger, M. Lahmann, T. K. Lindhorst, M. Marradi, P. Messner, A. Molinaro, P. V. Murphy, C. Nativi, S. Oscarson, S. Penadés, F. Peri, R. J. Pieters, O. Renaudet, J.-L. Reymond, B. Richichi, J. Rojo, F. Sansone, C. Schäffer, W. B. Turnbull, T. Velasco-Torrijos, S. Vidal, S. Vincent, T. Wennekes, H. Zuilhof, A. Imberty, *Chem. Soc. Rev.* **2013**, *42*, 4709–4727.

[59] C. White, A. Yates, P. M. Maitlis, D. M. Heinekey, John Wiley & Sons, Ltd, **2007**, pp. 228–234.

for Table of Contents entry only:

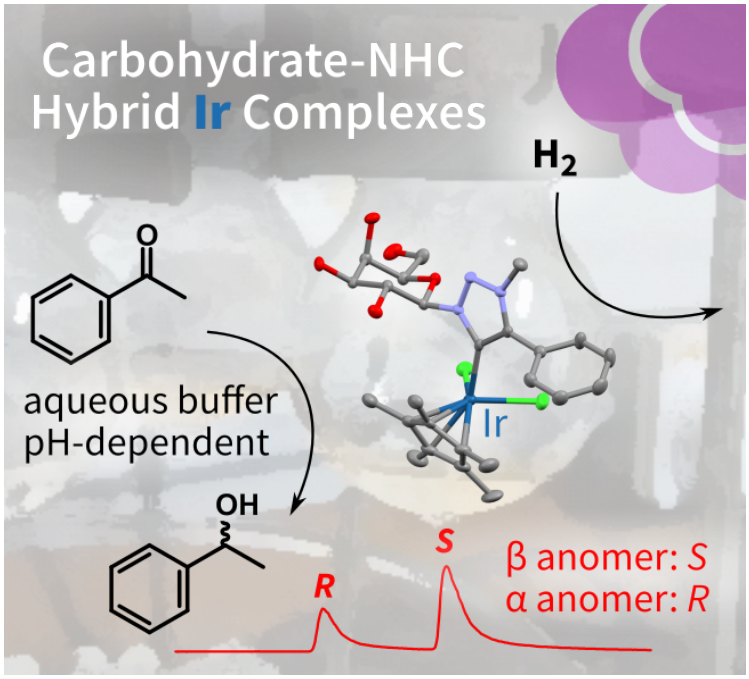

Iridium complexes containing a carbohydrate-functionalized N-heterocyclic carbene ligand impart pH-dependent catalytic activity in aqueous hydrogenation of ketones. The anomeric configuration is critical for directing the enantiopreference of hydrogenation, unveiling the dual role of the hybrid ligand in enabling catalytic activity and in directing stereoselectivity.